



## The use of micropatterning to control smooth muscle myosin heavy chain expression and limit the response to transforming growth factor $\beta$ 1 in vascular smooth muscle cells

Corin Williams<sup>a</sup>, Xin Q. Brown<sup>a</sup>, Erzsebet Bartolak-Suki<sup>a,b</sup>, Hongwei Ma<sup>c,1</sup>, Ashutosh Chilkoti<sup>c</sup>, Joyce Y. Wong<sup>a,\*</sup>

<sup>a</sup>Department of Biomedical Engineering, 44 Cummington St, Boston University, Boston, MA 02215, USA

<sup>b</sup>CelluTraf Sci. Inc, 49 Cragmore Rd, Newton, MA 02464, USA

<sup>c</sup>Department of Biomedical Engineering, Duke University, PO Box 90281, Durham, NC 27708, USA

### ARTICLE INFO

#### Article history:

Received 19 August 2010

Accepted 29 August 2010

Available online 19 September 2010

#### Keywords:

Micropatterning

Smooth muscle cell

Transforming growth factor  $\beta$  1

Arterial tissue engineering

### ABSTRACT

In the healthy artery, contractile vascular smooth muscle cells (VSMCs) have an elongated shape and are highly aligned but transition to a synthetic phenotype in culture, while additionally becoming well spread and randomly organized. Thus, controlling VSMC phenotype is a challenge in tissue engineering. In this study, we investigated the effects of micropatterning on contractile protein expression in VSMCs at low and high passage and in the presence of transforming growth factor beta 1 (TGF $\beta$ 1). Micropatterning led to significantly decreased cell area, increased elongation, and increased alignment compared to non-patterned VSMCs independent of passage number. In the presence of serum, micropatterning led to increased smooth muscle myosin heavy chain (SM-MHC) and  $\alpha$ -actin expression in low passage VSMCs, but had no effect on high passage VSMCs. Micropatterning was as effective as TGF $\beta$ 1 in up-regulating SM-MHC at low passage; however, micropatterning limited VSMC response to TGF $\beta$ 1 at both low and high passage. Investigation of TGF $\beta$  receptor 1 revealed higher expression in non-patterned VSMCs compared to patterned at high passage. Our studies demonstrate that micropatterning is an important regulator of SM-MHC expression in contractile VSMCs and that it may provide a mechanism for phenotype stabilization in the presence of growth factors.

© 2010 Elsevier Ltd. All rights reserved.

### 1. Introduction

Vascular smooth muscle cells (VSMCs) have an elongated shape and are circumferentially aligned within the medial layer of the healthy artery [1,2] in order to effectively regulate vessel distensibility and diameter [3]. Thus, VSMC shape and alignment may be critical to native artery function. Native VSMCs are generally considered to have a contractile phenotype, characterized by a well-developed contractile apparatus and high expression levels of proteins associated with contraction, such as smooth muscle myosin heavy chain (SM-MHC), smooth muscle  $\alpha$ -actin, basic calponin and SM22 $\alpha$  [4,5]. However, VSMCs also maintain phenotype plasticity at maturity [5,6], so that in response to injury or disease, VSMCs can dedifferentiate to a synthetic phenotype that is characterized by

migration, proliferation, decreased expression of contractile proteins, and increased synthesis of extracellular matrix (ECM) [6,7]. In culture, VSMCs inevitably modulate from the contractile to the synthetic phenotype [8,9], concurrently becoming highly spread and randomly oriented. Although phenotypic modulation is thought to be reversible both *in vivo* and *in vitro* [10–12], the synthetic phenotype dominates with increasing passage in culture.

The elucidation of factors involved in VSMC phenotype regulation is important not only for understanding the mechanisms that underlie cardiovascular disease progression, but is also critical for the successful development of functional tissue engineered vascular grafts (TEVGs). For example, the synthetic phenotype is advantageous to expand VSMC number for TEVG development; however, when the graft is ready for implantation, it would be desirable to revert VSMCs to their native contractile phenotype for proper graft function and to avoid uncontrolled proliferation that could lead to occlusion and TEVG failure.

Control of VSMC phenotype is a complex process that is dependent on numerous environmental cues, such as transforming growth factor beta 1 (TGF $\beta$ 1), platelet derived growth factor

\* Corresponding author. Tel.: +1 617 353 2374; fax: +1 617 353 6766.

E-mail address: [jywong@bu.edu](mailto:jywong@bu.edu) (J.Y. Wong).

<sup>1</sup> Present address. Suzhou Institute of Nano-Tech and Nano-Bionics, Chinese Academy of Sciences, 398 Ruo Shui Road, Suzhou Industrial Park, Suzhou, Jiangsu 215125, PR China.

(PDGF), ECM, mechanical forces, and cell–cell interactions [6]. Recently, studies have shown that micropatterned culture of VSMCs induces elongated shape and alignment [2,13–18], synthesis of organized fibronectin matrix [13], and decreased proliferation [2,18]. Studies from the Chan-Park group have reported increased contractile expression at confluence in VSMCs cultured in wide (160–300  $\mu\text{m}$ ) microchannels compared to flat substrates [14,19]. In this work, we aimed to further characterize the effects of micropatterning on VSMC contractile phenotype by investigating cells at low and high passage as well as in the presence of TGF $\beta$ 1. We expected that low passage, more contractile VSMCs may behave differently compared to high passage, more synthetic VSMCs on micropatterned substrates, as others have found phenotype-dependent responses in VSMCs to various cues [10,20–22]. Additionally, we asked whether micropatterning would affect VSMC response to TGF $\beta$ 1, a well-known stimulator of contractile protein expression in cultured cells [23–27]. Our micropatterned substrates consisted of narrow (20  $\mu\text{m}$ ) lanes separated by cell-resistant comb polymer barriers. To ensure that we were starting with a contractile population, we used VSMCs isolated from healthy rabbit arteries that were then cultured and passaged, leading to increasingly synthetic cells. As a measure of phenotype, we selected SM-MHC and  $\alpha$ -actin, as these proteins are major components of the contractile apparatus and are well-characterized markers of the contractile phenotype [4,6,28,29].

## 2. Materials and methods

### 2.1. Vascular smooth muscle cell isolation and culture

All procedures were performed in accordance with the Institutional Animal Care and Use Committee at Boston University and the NIH Guide for the Care and Use of Laboratory Animals. Healthy male New Zealand white rabbits (2.5–3 kg; Pine Acres Rabbitry, Brattleboro, VT) were euthanized with an overdose of sodium pentobarbital (>120 mg/kg) administered intravenously to the ear. Both left and right common carotid arteries were harvested using sterile tools. Vessels were immediately placed in cold Hank's Balanced Salt Solution (HBSS: 137 mM NaCl, 5.4 mM KCl, 0.42 mM Na<sub>2</sub>HPO<sub>4</sub>, 0.44 mM KH<sub>2</sub>PO<sub>4</sub>, 4.17 mM NaHCO<sub>3</sub>, 10 mM HEPES, 5.55 mM glucose; 1% penicillin–streptomycin; pH 7.4) and stored on ice until use (<1 h).

In order to obtain contractile VSMCs, cells were isolated from the harvested tissue by enzymatic digestion, modified from a previously published protocol [30]. Carotid arteries were first cleaned of excess surrounding tissue and the adventitia was removed. The vessels were cut open longitudinally and the intima was scraped with a cell scraper (BD Biosciences, San Jose, CA) to remove blood and endothelial cells. The tissue was then cut into approximately  $2 \times 2 \text{ mm}^2$  and underwent four separate incubations in digestion solution, designated T1 through T4, at 37 °C on a mechanical shaker. Serial incubations allowed for control of cell population purity and yield. The compositions and times of the digestions were as follows: T1 contained 200 U/ml collagenase (337 U/mg, Sigma, St. Louis, MO), 1.5 U/ml elastase (6.5 U/mg, Sigma), and 1.25% (w/v) trypsin inhibitor (Sigma) in HBSS, for 50–60 min; T2 and T3 each contained 100 U/ml collagenase, 1.5 U/ml elastase, and 1.25% trypsin inhibitor in HBSS, for 30–40 min; T4 contained 1.25% trypsin inhibitor in HBSS, for 30 min. In between incubations, the solution was passed through a Spectra/Mesh® polyester filter with a pore size of 300  $\mu\text{m}$  (Spectrum Labs, Rancho Dominguez, CA) and the tissue was rinsed with HBSS before transfer to the next digestion solution. Cells from T1 were discarded and cells from T2–T4 were plated into separate wells of a 6-well tissue culture plate (Corning, Lowell, MA). Cultured cells were given Dulbecco's Modified Eagle Medium (DMEM; Gibco® Invitrogen, Carlsbad, CA) supplemented with 10% bovine calf serum (BCS; Invitrogen), 1% L-glutamine, and 1% penicillin–streptomycin (Invitrogen). Medium was changed every 2–3 days and cells were passaged once confluent. Cells were used for experiments at primary culture and passages 1 and 5.

For these studies, please note the following definitions: freshly isolated VSMCs are those which have been harvested by enzymatic digestion but have not been cultured or exposed to serum (representative of the native contractile phenotype in the media); primary VSMCs are those which have been cultured but not passaged (representative of a more contractile phenotype in culture); and passaged VSMCs are those which have been sub-cultured from primary cells (passages 1 and 5, representative of an increasingly synthetic phenotype in culture).

### 2.2. Soft lithography for micropatterned stamps

Polydimethylsiloxane (PDMS) stamps were made according to soft lithography techniques [13]. Silicon wafers (Si-Tech Inc., Topsfield, MA) were cleaned with

acetone, methanol, and isopropanol, and dried with nitrogen gas. Wafers were baked for 5 min at 95 °C to ensure evaporation of solvents. Next, wafers were coated with SU8-2005 photoresist (Microchem Corp, Newton, MA) and spun at 2000 rpm for 120 s to obtain a photoresist layer with thickness of approximately 5  $\mu\text{m}$ . Wafers were pre-baked for 1 min at 65 °C, 2 min at 95 °C, and 1 min at 65 °C. Wafers were then exposed to UV light through a high-resolution transparency mask with desired pattern dimensions (CAD/Art Services, Bandon, OR) at 10 mW/cm<sup>2</sup> for 70 s. To dissolve unexposed photoresist, wafers were washed in SU8 Developer (Microchem Corp), resulting in the desired pattern on the wafer surface. Patterned wafers were treated with (heptafluoropropyl) trimethylsilane (Sigma) for 2 h to facilitate removal of PDMS. To fabricate stamps, PDMS pre-polymer and cross-linking agent (Sylgard 184, Corning) were mixed at a ratio of 10:1 and then cured against the wafer in an oven at 60 °C overnight. Stamps were cut from the wafer and used for microcontact printing ( $\mu\text{CP}$ ), as described below.

### 2.3. Microcontact printing of comb polymer for micropatterned cell culture

An amphiphilic comb polymer with a methyl methacrylate backbone and oligo ethylene glycol teeth [31] was used to make a protein- and cell-resistant pattern on tissue culture polystyrene (TCPS) or glass via  $\mu\text{CP}$ . The comb polymer was dissolved at 35 mg/ml in 80%/20% (v/v) ethanol/water mixture. Immediately prior to  $\mu\text{CP}$ , PDMS stamps were cleaned with acetone, methanol, and isopropanol and dried with air. Stamps then underwent air plasma treatment (Harrick PDC 32G, medium RF level, 45 s) to render the surfaces hydrophilic. Approximately 200  $\mu\text{l}$  of comb polymer solution was immediately spread on the stamp surface and spun at 2000 rpm for 15 s (Model P6700, Specialty Coating Systems, Indianapolis, IN), resulting in a thin, dried layer of the comb polymer. The stamp was then immediately brought into conformal contact with the TCPS or glass surface, pressed firmly, and carefully peeled away. The comb polymer was annealed in an oven overnight at 60 °C. Substrates that were not to be used the same day were covered with phosphate buffered saline (PBS; Invitrogen) and stored at 4 °C (<2 wk). Prior to cell seeding, patterned substrates were covered with distilled water for 1–2 h at room temperature (RT) to reorient the comb polymer, and then washed 3 times with sterile PBS pre-warmed to 37 °C. Primary, non-passaged VSMCs were seeded directly onto patterned substrates after enzymatic dissociation. For passaged VSMC experiments, cells were sub-cultured on standard (i.e., non-patterned) TCPS dishes, trypsinized, and seeded onto patterned substrates at the desired passage number. Comb polymer patterns served as barriers that prevented cell adhesion in the printed regions; thus cell adhesion was to the exposed TCPS or glass surface only. A schematic for  $\mu\text{CP}$  of the comb polymer pattern and a representative phase contrast image of cells on a patterned TCPS substrate are shown in Fig. 1, panels A & B, respectively.

### 2.4. Characterization of cell morphology and alignment

To determine the effect of lane width on primary and passaged VSMC area, shape, and alignment, stamps with 10, 20, and 40  $\mu\text{m}$ -wide grooves and 100  $\mu\text{m}$ -wide ridges were used to  $\mu\text{CP}$  comb polymer patterns onto TCPS. Non-patterned substrates served as controls. For these studies, sub-confluent samples were used in order to easily distinguish individual cells. Phase contrast images at 10 $\times$  magnification were acquired for multiple, random fields using an Axiovert S-100 microscope (Carl Zeiss, Inc.) and Metamorph imaging software. We characterized morphology by two parameters: cell area and cell shape index (CSI). Cell borders were outlined using ImageJ 1.37v software (NIH, Bethesda, MD) and cell area (A) and perimeter (P) were measured. Cell shape was calculated according to the following formula:  $\text{CSI} = 4\pi A/P^2$ ; as  $\text{CSI} \rightarrow 0$ , cells become infinitely elongated and as  $\text{CSI} \rightarrow 1$ , cells become perfectly circular [2]. Cell alignment was measured through the long axis of the cell with respect to the pattern direction or, in the case of non-patterned controls, with respect to an arbitrary direction. Angles were measured such that a cell which was aligned perfectly parallel to the pattern/arbitrary direction had an orientation of 0° and perfectly perpendicular as 90°. A cell was considered aligned if it was oriented within 5° of the pattern or arbitrary direction, and the percentage of aligned cells was calculated based on this definition. Fifty cells were analyzed per sample; the criteria for inclusion in the analysis were as follows: 1) the individual cell outline was distinguishable and 2) for patterned cells, the cell was attached within a single lane (e.g., cells that bridged the comb polymer to attach in two lanes or cells that were attached in defective regions of the pattern were excluded). Note that primary, non-passaged VSMCs were used only for these initial studies of lane width effects; all further experiments used passaged VSMCs.

### 2.5. Cell manipulations for Western blot studies

Samples to be used for Western blot were prepared as follows. Stamps with 20  $\mu\text{m}$ -wide grooves and 50  $\mu\text{m}$ -wide ridges were used to fully pattern one surface of 25 mm circular cover slips (No. 1; VWR, West Chester, PA). A narrower comb polymer barrier was used to increase the number of cells per sample while still limiting bridging behavior of cells across the comb polymer. Cover slips were placed into individual wells of 6-well plates for cell culture.

VSMCs at passages 1 and 5 were seeded at moderate density in 10% BCS-containing DMEM such that the samples became confluent within 3–4 days. Note that

for patterned samples, confluence was restricted to the lanes between comb polymer barriers. Prior to lysis, cells were imaged to determine area, shape, and alignment, as described above. To avoid mixed populations (i.e., non-patterned cells attached to the bottom of TCPS wells), glass cover slip samples were transferred to new 6-well plates and washed with PBS. Cells were then collected in lysis buffer (20 mM Tris, 5 mM EDTA, 1% (v/v) TritonX-100, 150 mM NaCl, 5 mM EETA, pH = 7.4) with 1 mM phenylmethanesulfonyl fluoride (PMSF; Sigma), 0.2 mM Na<sub>2</sub>VO<sub>4</sub>, and protease inhibitor cocktail (Sigma) at 1:500 dilution added fresh before use. Samples were vortexed, incubated for 5 min on ice, and spun at 15,000 rpm for 15 min at 4 °C. The supernatant from each sample was transferred to a new microcentrifuge tube and stored at –20 °C until use.

For TGFβ1 studies, cells were seeded at high density in 10% BCS-containing DMEM overnight such that cells were confluent the next day. Cells were serum-starved overnight and then treated with a single dose of 10 ng/ml TGFβ1 (R&D Systems, Minneapolis, MN) in fresh serum-free DMEM or no TGFβ1 (control) overnight. After 24 h, cells were lysed, as described above.

## 2.6. Western blot for contractile marker proteins

To determine the effect of micropatterning on passaged VSMC contractile phenotype, we analyzed SM-MHC and smooth muscle α-actin expression levels using Western blot. Freshly dissociated VSMCs were lysed immediately after isolation from tissue and served as positive controls. Total protein was determined using a bicinchoninic acid (BCA) assay (Pierce, Rockford, IL), with each sample run in triplicate. Equal amounts of protein for each sample set (with the exception of freshly dissociated VSMCs) were separated by SDS-PAGE using 7.5% polyacrylamide gels. Due to the high signals for contractile proteins in freshly dissociated VSMCs, less protein was loaded for these samples (approximately half, compared to passaged VSMCs). Further, we note here that the data were not normalized to a load control because we have not found an appropriate load control for VSMCs of different phenotypes; proteins that are commonly probed as load controls (such as β-actin or α-tubulin) are known to change with VSMC phenotype [8,10,32]. Proteins were transferred to polyvinylidene difluoride (PVDF) membranes (Millipore, Billerica, MA) and blocked with 5% Carnation non-fat dry milk dissolved in Tris buffered saline with Tween 20 (TBST) for 1 h at RT. Mouse monoclonal SM-MHC (clone SMMS-1; DAKO, Denmark) and α-actin (clone 1A4, Sigma) primary antibodies were incubated with membranes using optimized dilutions at 4 °C overnight (1:2000 and 1:5000 for SM-MHC and α-actin, respectively). After washing with TBST, membranes were incubated with optimized dilutions of horse radish peroxidase (HRP)-conjugated goat anti-mouse IgG (Zymed, S. San Francisco, CA; 1:10,000 and 1:50,000 for SM-MHC and α-actin, respectively) for 30 min at RT. The membranes were again washed, and then reacted with SuperSignal West Pico Chemiluminescent Substrate (Pierce). Signals were captured on film (GE Life Sciences, Piscataway, NJ), developed, and analyzed using ImageJ's gel plug-in. The raw data were normalized such that the non-patterned mean was adjusted to unity and the patterned mean showed relative change compared to non-patterned. For TGFβ1 studies, TGFβ receptor 1 (TGFβR1) expression was also determined by Western blot, as described above. Goat polyclonal TGFβR1 primary antibody (Santa Cruz Biotechnology, Santa Cruz, CA) was used at a dilution of 1:500 and HRP-conjugated donkey anti-goat IgG (Santa Cruz) was used at a dilution of 1:20,000. For all experiments, samples were run in triplicate.

## 2.7. Statistical analysis

For the study of lane width effects on VSMCs area and shape, statistical significance was determined within primary and passaged groups using one-way analysis of variance (ANOVA) and Tukey's post-hoc test. These tests were also used for comparing multiple conditions in TGFβ1 experiments. In the case where only two

conditions were compared (e.g., non-patterned primary vs. non-patterned passaged VSMC area/shape, protein expression in patterned vs. non-patterned VSMCs), the Student's *t*-test was used. A statistically significant difference was considered to exist for a *p*-value less than 0.05.

## 3. Results

### 3.1. Morphology and alignment of micropatterned VSMCs

The initial goal of our study was to determine whether micropatterning could modulate the morphology and alignment of passaged, more synthetic VSMCs to mimic primary, more contractile VSMCs. Primary and passaged VSMCs were seeded at sub-confluence onto non-patterned substrates and patterns with 40, 20, or 10 μm-wide lanes (Fig. 2A). Micropatterning had no effect on primary VSMC area, but significantly decreased passaged VSMC area to values similar to primary VSMCs on 20 and 10 μm-wide lanes (Fig. 2B). Although primary VSMCs were more elongated than passaged VSMCs on non-patterned substrates, patterned primary and passaged VSMCs had the same CSI, which decreased significantly as lane width decreased (Fig. 2C). Further, both primary and passaged VSMCs became increasingly aligned as lane width decreased (Fig. 2D).

Overall, we found that sub-confluent primary and passaged VSMCs had the same morphology and alignment on 20 and 10 μm-wide lanes. As 20 μm-wide lanes were the less restrictive of the two patterns that resulted in the desired effect, we chose this pattern for all subsequent studies.

As passaged VSMCs grow to confluence, they assume a more elongated shape and develop regions of local alignment. Therefore, we next asked whether the effect of micropatterning on cell morphology and alignment was simply a result of mimicking the condition of high confluence. Although non-patterned VSMC area decreased from 5190 ± 2220 μm<sup>2</sup> at sub-confluence (Fig. 2B) to 1450 ± 686 μm<sup>2</sup> at confluence (Fig. 3B), cells cultured on 20 μm-wide lanes at confluence exhibited significantly smaller area (890 ± 360 μm<sup>2</sup>) and more elongated shape (CSI = 0.18 ± 0.06; Fig. 2C) compared to confluent non-patterned cells. Moreover, confluent non-patterned VSMCs remained overall randomly oriented while micropatterning induced high alignment at confluence (Fig. 3D).

We also investigated whether micropatterning was equally effective for low passage (more contractile) and high passage (more synthetic) VSMCs. When comparing passage 1 vs. passage 5, we noted that for both cases patterned VSMCs were significantly smaller, more elongated, and more aligned compared to non-patterned VSMCs. However, there was no difference in patterned passage 1 VSMC morphology and alignment vs. patterned passage 5; additionally, there was no difference between non-patterned

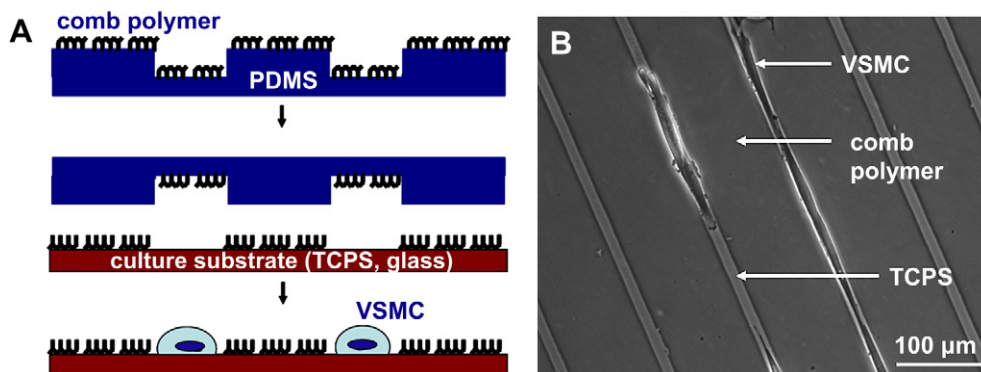


**Fig. 1.** Micropatterning to control VSMC shape and organization using microcontact printed comb polymer patterns. (A) Comb polymer solution is spun-cast onto a polydimethylsiloxane (PDMS) stamp and printed onto the cell culture substrate. The comb polymer acts as a protein- and cell-resistant barrier: cell attachment is restricted to exposed (non-printed) regions. (B) Representative phase contrast image of VSMCs in 10 μm-wide lanes of tissue culture polystyrene (TCPS) with 100 μm-wide comb polymer barriers.

passage 1 vs. passage 5 VSMCs. All together, these results demonstrate that micropatterning has a greater effect on VSMC morphology and alignment than high confluence alone; further, micropatterning had the same effect on morphology and alignment at passage 1 and passage 5.

### 3.2. SM-MHC and $\alpha$ -actin expression in micropatterned VSMCs

Having determined the effects of micropatterning on VSMC morphology and alignment at passages of interest, we then investigated its effect on VSMC contractile protein expression. Other studies have shown phenotype- or passage-dependent changes in proteins in VSMCs [10,33] as well as in VSMC response to different factors [21,22]. Therefore, we suspected that the effects of micropatterning may also depend on the passage number or initial phenotypic state of VSMCs. Cells at passages 1 and 5 were cultured with 10% serum-containing medium on non-patterned and patterned substrates and lysed at confluence for Western blot analysis. At passage 1, patterned VSMCs had significantly higher expression of SM-MHC and  $\alpha$ -actin compared to non-patterned VSMCs ( $2.1 \pm 0.4$  and  $2.3 \pm 0.5$ -fold relative increase, respectively); however, these differences disappeared at passage 5 (Fig. 4). Interestingly, when compared to freshly isolated, native VSMCs,  $\alpha$ -actin expression in non-patterned passage 1 VSMCs was decreased ( $49 \pm 11\%$  of native VSMC expression) while patterned passage 1 VSMCs had equivalent expression ( $106 \pm 28\%$ ). SM-MHC was quickly down-regulated to approximately 10% of native levels in

primary confluent VSMCs in standard (i.e., non-patterned) culture; at passage 1, non-patterned VSMCs had further down-regulation to  $4.8 \pm 0.7\%$  while patterned VSMCs had expression similar to primary VSMCs ( $9.2 \pm 1.8\%$ ). These observations show that micropatterning prevented further down-regulation of contractile proteins from primary culture to first passage. Further, we note that while the effects of micropatterning are passage-dependent, they are not due to changes in morphology or alignment with increasing passage (Fig. 3).

### 3.3. TGF $\beta$ 1 stimulation in micropatterned VSMCs

TGF $\beta$ 1 has been shown to increase the expression of smooth muscle-specific genes, including SM-MHC and  $\alpha$ -actin, in cultured VSMCs [27]. We therefore investigated the combined effects of micropatterning and TGF $\beta$ 1 treatment on SM-MHC and  $\alpha$ -actin expression in passaged VSMCs. To ensure that no competing influences were present, experiments were carried out with confluent cells under serum-free conditions. VSMCs were stimulated with a single dose of TGF $\beta$ 1 at 10 ng/ml or no TGF $\beta$ 1 as a control and lysed after 24 h. TGF $\beta$ 1 significantly increased SM-MHC expression in non-patterned VSMCs under serum-free conditions, as reported by others [27,34]. Similar to serum-containing conditions, micropatterning significantly increased SM-MHC expression, and levels were comparable to TGF $\beta$ 1-treated cells (Fig. 5A and B). However, micropatterning and TGF $\beta$ 1 treatment did not have an additive effect on SM-MHC expression in

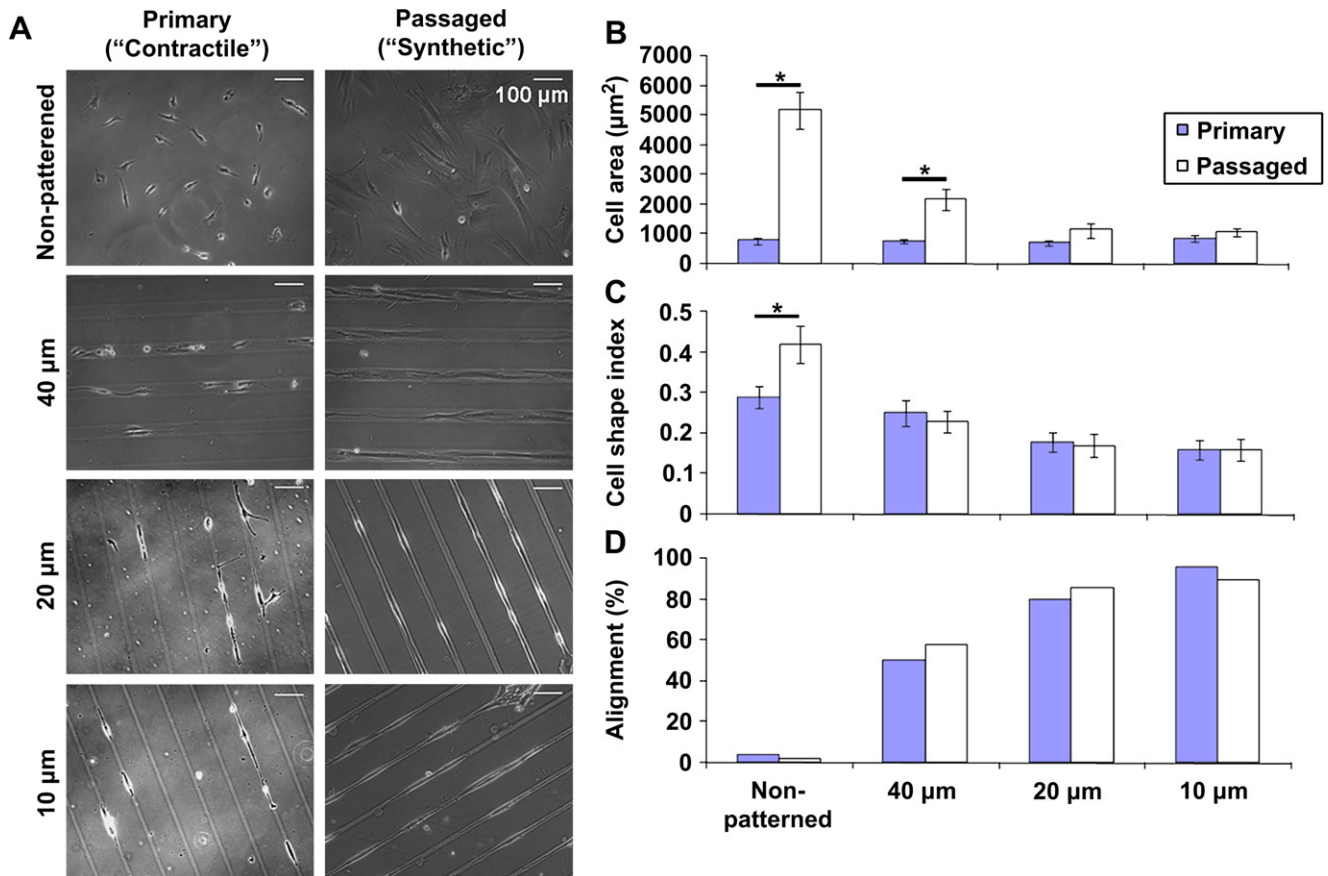


**Fig. 2.** Micropatterning leads to similar morphology and alignment in primary and passaged VSMCs. (A) Representative phase contrast images of sub-confluent primary, non-passaged (more contractile) and passaged (more synthetic) VSMCs. (B) Primary VSMC area (solid) was unaffected by patterning while passaged VSMC area (open) decreased with decreasing lane width. (C) Primary and passaged VSMCs became increasingly elongated in shape with decreasing lane width. (D) Primary and passaged VSMCs became increasingly aligned within  $5^\circ$  of the pattern as lane width decreased; non-patterned VSMCs had no preferred orientation. B and C show mean  $\pm$  2SEM for  $n = 50$  cells per condition. \* indicates significant difference for  $p < 0.05$ .

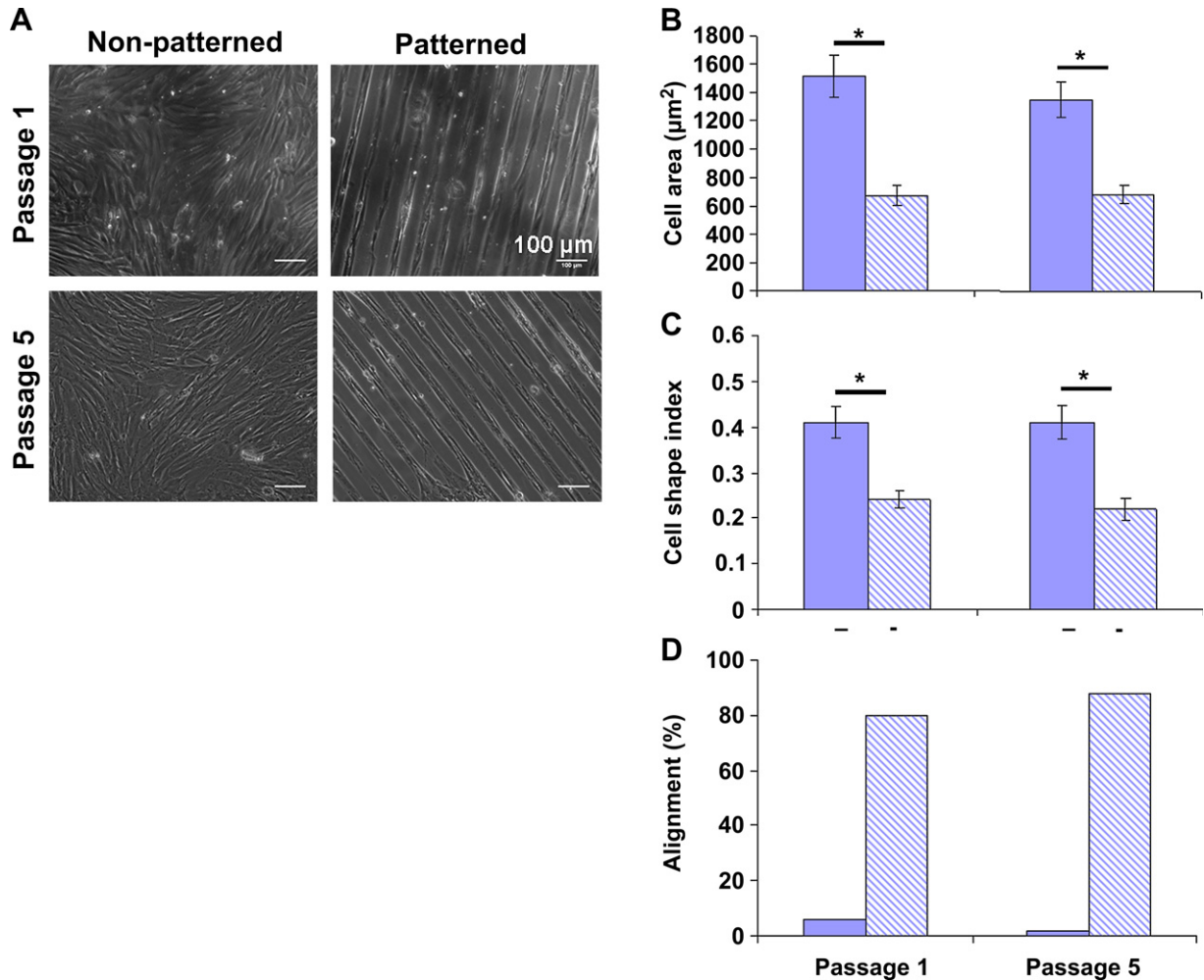


**Fig. 3.** The effects of micropatterning on morphology and alignment are maintained at confluence and with increasing passage. (A) Representative images of confluent samples at passages 1 and 5 on non-patterned and patterned substrates. (B) Cell area and (C) shape did not change in non-patterned VSMCs (solid) from passages 1 to 5; this was also true for patterned VSMCs (striped). However, patterned VSMCs were significantly smaller and more elongated compared to non-patterned VSMCs for both passages studied. (D) Orientation did not change with passage: non-patterned VSMCs remained randomly oriented and patterned VSMCs remained highly aligned with the pattern. Data in B and C are mean  $\pm$  2SEM for  $n = 50$  cells per condition. \* indicates significant difference for  $p < 0.05$ .

passage 1 VSMCs. Serum starvation led to similar expression of  $\alpha$ -actin in patterned and non-patterned VSMCs, and stimulation with TGF $\beta$ 1 had no effect (Fig. 5A and C). These findings demonstrate that micropatterning is as effective as TGF $\beta$ 1 treatment in up-regulating SM-MHC expression in passage 1 VSMCs. Further, our results show that the effect of micropatterning on SM-MHC expression is independent of the presence of serum or exogenous growth factors; on the other hand, the effect of micropatterning on  $\alpha$ -actin expression was dependent on serum, but not TGF $\beta$ 1.

Because we observed different responses to micropatterning at passage 1 and passage 5 in our initial phenotype studies, it was likely that the response to TGF $\beta$ 1 would also differ in passage 1 vs. passage 5 VSMCs. In serum-starved, non-treated VSMCs at passage 5, there was no difference in SM-MHC expression in non-patterned and patterned VSMCs (Fig. 6A and B), similar to serum-containing conditions (Fig. 4A and B). TGF $\beta$ 1 stimulation led to significantly higher levels ( $2.2 \pm 0.4$ -fold) of SM-MHC expression compared to patterned VSMCs. TGF $\beta$ 1 did not alter SM-MHC expression in patterned VSMCs at passage 5, as found with patterned passage 1 VSMCs, suggesting that micropatterning inhibits the TGF $\beta$ 1-induced increase of SM-MHC. Similar to the findings in TGF $\beta$ 1 studies at passage 1, there was no effect of serum starvation or

TGF $\beta$ 1 treatment on  $\alpha$ -actin expression in non-patterned and patterned VSMCs at passage 5 (Fig. 6C).

#### 3.4. TGF $\beta$ 1 expression in micropatterned VSMCs

To gain insight into how micropatterning may inhibit VSMC response to TGF $\beta$ 1, we investigated TGF $\beta$  receptor 1 (TGF $\beta$ R1) expression in VSMCs at passages 1 and 5. There was no difference in TGF $\beta$ R1 expression in non-patterned vs. patterned VSMCs at passage 1; however, at passage 5, TGF $\beta$ R1 was significantly lower in patterned VSMCs compared to non-patterned (Fig. 7). In fact, TGF $\beta$ R1 was  $2.2 \pm 0.4$ -fold higher in passage 5 non-patterned VSMCs compared to patterned VSMCs, similar to the fold-increase in SM-MHC as a result of TGF $\beta$ 1 stimulation at passage 5. Lower TGF $\beta$ R1 expression in patterned VSMCs relative to non-patterned VSMCs suggests that micropatterning may limit TGF $\beta$ 1 signaling via TGF $\beta$ R1.

## 4. Discussion

VSMCs convert from the native contractile phenotype to a synthetic phenotype in culture; controlling this behavior is a challenge for basic VSMC research and vascular tissue

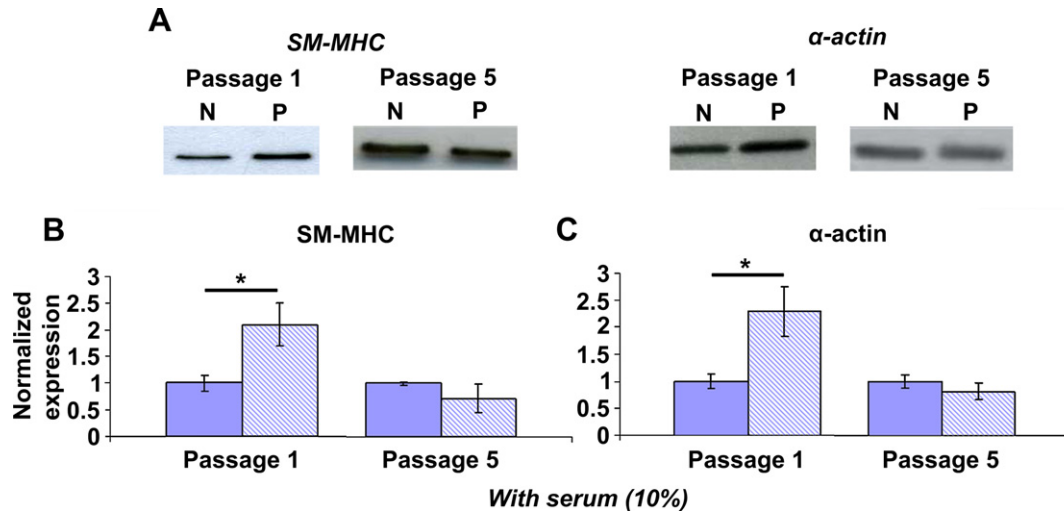


**Fig. 4.** Micropatterning leads to increased SM-MHC and  $\alpha$ -actin at passage 1 but not at passage 5. (A) Representative blots for non-patterned (N) and patterned (P) VSMCs at passages 1 and 5. All samples were confluent and cultured with 10% serum. (B) SM-MHC and (C)  $\alpha$ -actin expression were significantly higher in patterned vs. non-patterned VSMCs at passage 5. B and C show mean  $\pm$  SD for  $n = 3$ . The non-patterned means are normalized to unity and the patterned means are expressed as a relative change. \* indicates significant difference for  $p < 0.05$ .

engineering. While modulation to the synthetic phenotype is a well-characterized phenomenon, the factors that may maintain, preserve, or enhance the contractile phenotype are less understood, but would provide valuable guidance to the design of functional TEVGs. Despite numerous approaches to mimic native VSMC shape and organization in culture, our knowledge to date regarding the effects of micropatterning on VSMC phenotype is still limited. Therefore, our studies aimed to characterize the effects of micropatterning on the contractile marker proteins SM-MHC and  $\alpha$ -actin in cultured VSMCs at different passages and in the presence of TGF $\beta$ 1. We found that micropatterning had significantly different effects on contractile protein expression at passages 1 and 5, despite inducing the same morphology and alignment at these passages. Further, we found that although micropatterning was as effective as TGF $\beta$ 1 stimulation in up-regulating SM-MHC, it limited VSMC response to TGF $\beta$ 1 due to a relative decrease of TGF $\beta$ 1R1

compared to non-patterned VSMCs. These results have interesting implications for future *in vitro* studies of VSMC behavior as well as the role of micropatterning on VSMC phenotype in native arteries and TEVGs *in vivo*.

Our observation that micropatterning had different effects on SM-MHC and  $\alpha$ -actin expression at passages 1 and 5, despite having the same effect on morphology and alignment, suggests that its influence on protein expression depends on the initial phenotype of the VSMC. Perhaps VSMCs have memory of the contractile phenotype that is lost at higher passages. As VSMCs become increasingly synthetic in culture, a VSMC at passage 1 is presumably more contractile than a VSMC at passage 5. It is likely that micropatterning is an important regulator of phenotype in VSMCs which are already in a more contractile state. This may occur *in vivo*, where the majority of VSMCs, which have an elongated shape and are highly aligned within the media, maintain the contractile

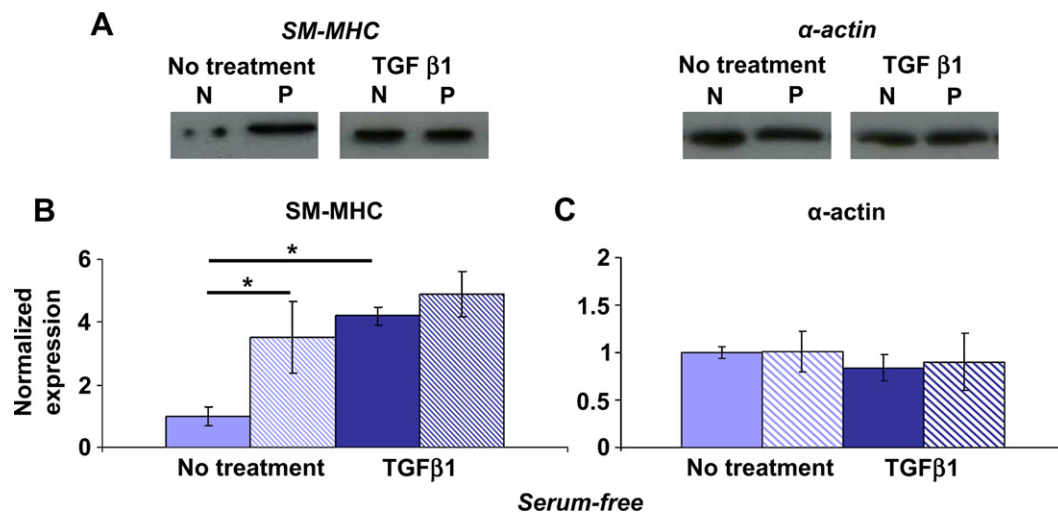


**Fig. 5.** Micropatterning is as effective as TGF $\beta$ 1 stimulation in up-regulating SM-MHC expression at passage 1. (A) Representative blots for non-patterned (N) and patterned (P) VSMCs at passage 1, without treatment or with 10 ng/ml TGF $\beta$ 1 stimulation overnight under serum-free conditions. (B) SM-MHC was significantly higher in non-treated patterned VSMCs (striped) compared to non-patterned (solid). Treatment with TGF $\beta$ 1 led to significant increase in SM-MHC in non-patterned VSMCs such that there was no difference compared to patterned VSMCs. (C)  $\alpha$ -actin expression was similar in patterned and non-patterned VSMCs both for non-treated and TGF $\beta$ 1-treated conditions. B and C show mean  $\pm$  SD for  $n = 3$ , where the non-patterned, non-treated means are normalized to unity and all other conditions are expressed as a relative change. \* indicates significant difference for  $p < 0.05$ .

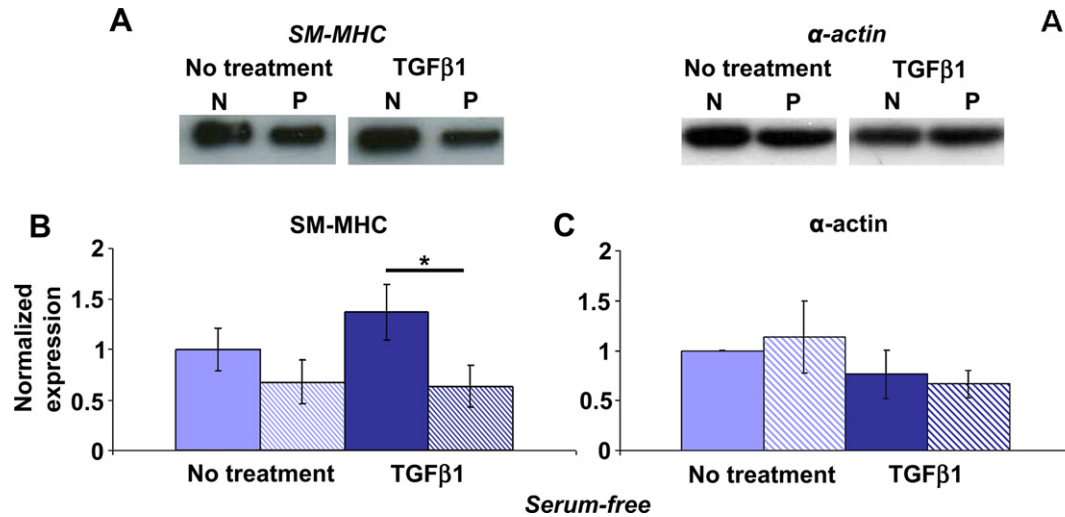


**Fig. 6.** Micro patterning limits VSMC response to TGFβ1 stimulation at passage 5. (A) Representative blots for non-patterned (N) and patterned (P) VSMCs, without treatment or with 10 ng/ml TGFβ1 stimulation overnight under serum-free conditions. (B) SM-MHC was significantly higher in non-patterned VSMCs (solid) vs. patterned VSMCs (striped) stimulated with TGFβ1. (C) TGFβ1 stimulation did not result in a significant difference in α-actin expression in non-patterned vs. patterned VSMCs. B and C show mean ± SD for  $n = 3$ . The non-treated, non-patterned means are normalized to unity and all other conditions are expressed as a relative change. \* indicates significant difference for  $p < 0.05$ .

phenotype [1,6]. Once VSMCs become synthetic, micropatterning may be overcome by competing factors that promote the synthetic phenotype. This could explain why the neointima that forms during the aging process can contain highly aligned layers of VSMCs [35] and yet continue to thicken [35,36]. Phenotype-dependent responses to the same environmental cue are an intriguing but not well-understood phenomenon, although a few studies have highlighted their importance [21,22]. Future investigations to determine the mechanisms that govern VSMC phenotype memory and phenotype-dependent responses will be critical to gaining deeper knowledge of VSMC behavior in health and disease, as well as for informing the development of TEVGs. Our findings here suggest that low passage VSMCs should be used in TEVGs in order to have a phenotype advantage (i.e., more contractile cells) that leads to better vasoactive function as well as to avoid excessive or

potentially irreversible modulation to the synthetic phenotype that could lead to graft occlusion. Alternatively, it is of interest in future work to determine whether repeated passage of VSMCs on micropatterned substrates from primary culture or first passage can maintain increased levels of SM-MHC and α-actin indefinitely, potentially allowing for expansion of contractile VSMCs that can be used to populate a TEVG (Fig. 8).

Stimulation of VSMCs with TGFβ1 yielded further insight into the influence of micropatterning on VSMC phenotype. TGFβ1 has been shown to increase SM-MHC and α-actin gene expression in cultured VSMCs [27,34] and evidence suggests that it is an important regulator of VSMC phenotype *in vivo* [6,37–39]. We found that TGFβ1 resulted in increased SM-MHC in non-patterned VSMCs, but had no effect on α-actin. Interestingly, micropatterning and TGFβ1 stimulation were equally effective in up-regulating SM-MHC expression at passage 1. Further, we note that SM-MHC was significantly higher in patterned VSMCs compared to non-patterned VSMCs under both serum-containing and serum-free conditions; taken together with the observation that SM-MHC did not increase in patterned VSMCs stimulated with TGFβ1, our findings suggest that micropatterning is a potent regulator of SM-MHC expression independent of the presence of other factors. TGFβ1 has been used in other vascular tissue engineering studies to modulate VSMC behavior [40,41]. However, micropatterning may be a more useful approach than TGFβ1 stimulation for developing functional TEVGs, since micropatterning induces elongated shape and alignment similar to native VSMCs in addition to maintaining a more contractile phenotype in low passage VSMCs.

At both passages 1 and 5, TGFβ1 had no effect on patterned VSMCs while it resulted in increased SM-MHC in non-patterned VSMCs. This can be explained, in part, by TGFβR1 expression. Although TGFβR1 does not directly bind TGFβ1, it acts as a mediator via recruitment to TGFβ1-bound TGFβR2, and subsequently induces downstream signaling of TGFβ1 pathways [42,43]. At passage 1, there was no significant difference between patterned and non-patterned TGFβR1 expression. Although SM-MHC expression was significantly higher in patterned VSMCs compared to non-patterned, there was no change in TGFβ1-stimulated vs. non-stimulated patterned VSMCs. We propose this could be due to one or more of the following: 1) SM-MHC expression levels cannot be induced to increase further due to regulation by micropatterning, or 2) micropatterning interferes with the

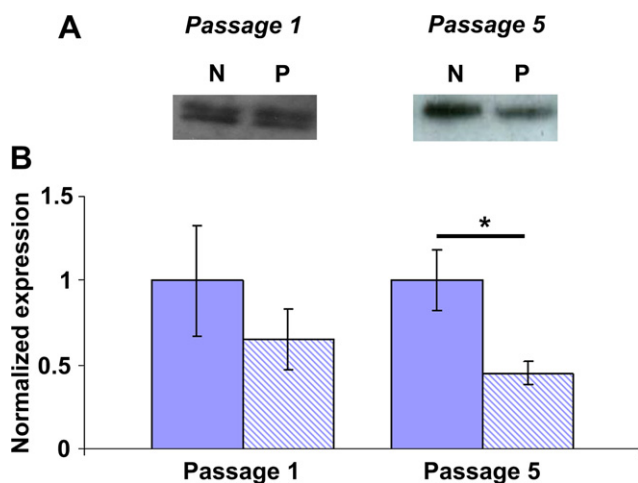


**Fig. 7.** Micropatterning results in decreased TGFβR1 expression in VSMCs at passage 5. (A) Representative blots of TGFβR1 for serum-starved non-patterned (N) and patterned (P) VSMCs at passages 1 and 5. (B) There was no significant difference in TGFβR1 expression at passage 1 for non-patterned (solid) vs. patterned (striped) VSMCs. At passage 5, TGFβR1 was significantly lower in patterned VSMCs compared to non-patterned. B shows mean ± SD for  $n = 3$ , where the non-patterned means are normalized to unity and patterned means are expressed as a relative change. \* indicates significant difference for  $p < 0.05$ .

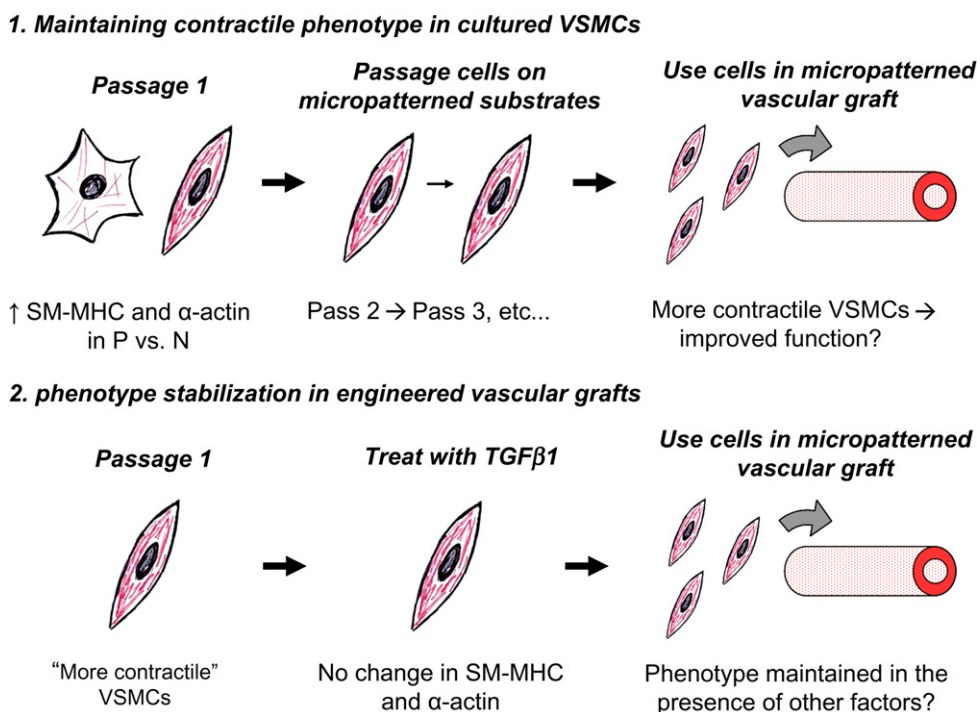


**Fig. 8.** Micropatterning to control VSMC behavior for the development of functional tissue engineered vascular grafts. Cartoons depict potential applications of micropatterning based on data presented in Figs. 4–7. See Discussion text for details.

ability of TGF $\beta$ 1 to bind receptors or otherwise allow proper signaling. At passage 5, the explanation is more straightforward: a 2-fold higher expression of TGF $\beta$ R1 in non-patterned VSMCs correlates to a 2-fold higher expression of SM-MHC in non-patterned VSMCs compared to patterned VSMCs with TGF $\beta$ 1 stimulation. Because TGF $\beta$ R1 expression is effectively lower with micropatterning, TGF $\beta$ 1-mediated activation of the TGF $\beta$ 1 signaling pathway is limited, although other influences may also play a role.

The resistance of patterned VSMCs to growth factor stimulation implies a useful function of micropatterning that may be exploited in TEVGs. It is likely that other growth factor receptors in addition to TGF $\beta$ R1 are controlled through micropatterning, providing VSMCs with a mechanism for phenotype stabilization. This is further supported by our preliminary results with PDGF, which is known to down-regulate contractile proteins in culture [44]. Patterned VSMCs at passage 5 showed no response 24 h after stimulation with PDGF-BB (10 ng/ml); in fact, there was no change in SM-MHC or  $\alpha$ -actin expression in patterned VSMCs stimulated with PDGF compared to TGF $\beta$ 1 (data not shown). *In vivo*, VSMCs are exposed to a myriad of changing factors and signals that can potentially perturb their phenotype; nevertheless, these cells remain in the contractile phenotype in the healthy artery. The micropatterning that naturally occurs in the media may serve not only to maximize VSMC contractile functions but to help regulate cell response and stabilize phenotype. In creating TEVGs, it would be desirable to populate the graft with contractile VSMCs that will be resistant to phenotype perturbations once implanted *in vivo* to ensure proper graft function. Our findings imply that incorporation of micropatterned cues into the TEVG may be a powerful method for controlling and maintaining the contractile VSMC phenotype (Fig. 8).

## 5. Conclusions

In this study, we characterized the effects of micropatterning on cultured VSMC phenotype at different passages and with

TGF $\beta$ 1 stimulation. Micropatterned substrates consisting of 20  $\mu$ m-wide lanes induced similar morphology and alignment in primary, contractile VSMCs and passaged, synthetic VSMCs. Micropatterning led to significantly higher expression of SM-MHC and  $\alpha$ -actin at passage 1 but had no effect at passage 5. Additionally, micropatterning was as effective as TGF $\beta$ 1 stimulation in up-regulating SM-MHC expression; however, patterned VSMC response to TGF $\beta$ 1 was limited due to a relative decrease of TGF $\beta$ R1 compared to non-patterned VSMCs. Our findings have shed light on the utility of micropatterning to control VSMC behavior *in vitro* as well as providing intriguing implications for its use in TEVGs to be implanted *in vivo*. Like most *in vitro* systems, our approach is an artificial attempt to recapitulate one aspect of the native environment that influences VSMCs, as it is impossible to recreate the numerous cues present in the artery. Likely, other factors will need to be considered in the design of TEVGs. Additional studies to elucidate the mechanisms by which micropatterning modulates VSMC phenotype will yield further insight into the benefits and limitations of using micropatterning techniques to control VSMC behavior for vascular tissue engineering applications.

## Acknowledgements

We are grateful to Prof. Kathleen G. Morgan (Boston University) for her insightful discussions regarding the data and manuscript. This work was supported by the NIH National Heart, Lung, and Blood Institute R01 HL72900 (J.Y.W.).

## Appendix

Figures with essential color discrimination. Figs. 1–8 in this article are difficult to interpret in black and white. The full color images can be found in the on-line version, at [doi:10.1016/j.biomaterials.2010.08.105](https://doi.org/10.1016/j.biomaterials.2010.08.105).

## References

- [1] Krizmanich WJ, Lee RMKW. Correlation of vascular smooth muscle cell morphology observed by scanning electron microscopy with transmission electron microscopy. *Exp Mol Pathol* 1997;64:157–72.
- [2] Thakar RG, Ho F, Huang NF, Liepmann D, Li S. Regulation of vascular smooth muscle cells by micropatterning. *Biochem Biophys Res Commun* 2003;307:883–90.
- [3] Holzapfel GA, Ogden RW, editors. *Biomechanics of soft tissue in cardiovascular systems*. New York: Springer-Verlag; 2003.
- [4] Owens GK. Regulation of differentiation of vascular smooth muscle cells. *Physiol Rev* 1995;75:487–517.
- [5] Rzucidlo EM, Martin KA, Powell RJ. Regulation of vascular smooth muscle cell differentiation. *J Vasc Res* 2007;45:25A–32A.
- [6] Owens GK, Kumar MS, Wamhoff BR. Molecular regulation of vascular smooth muscle cell differentiation in development and disease. *Physiol Rev* 2004;84:767–801.
- [7] Birukov KG, Frid MG, Rogers JD, Shirinsky VP, Koteliansky VE, Campbell JH, et al. Synthesis and expression of smooth muscle phenotype markers in primary culture of rabbit aortic smooth muscle cells: influence of seeding density and media and relation to cell contractility. *Exp Cell Res* 1993;204:46–53.
- [8] Pauly RR, Bilato C, Cheng L, Monticone R, Crow MT. Vascular smooth muscle cell cultures. *Methods Cell Biol* 1998;52:133–54.
- [9] Chamley-Campbell J, Campbell GR, Ross R. The smooth muscle cell in culture. *Physiol Rev* 1979;59:1–61.
- [10] Worth NF, Rolfe BE, Song J, Campbell GR. Vascular smooth muscle cell phenotypic modulation in culture is associated with reorganisation of contractile and cytoskeletal proteins. *Cell Motil Cytoskeleton* 2001;49:130–45.
- [11] Absher M, Woodcock-Mitchell J, Mitchell J, Baldor L, Low R, Warshaw D. Characterization of vascular smooth muscle cell phenotype in long-term culture. *In Vitro Cell Dev Biol* 1989;25(2):183–92.
- [12] Li S, Sims S, Jiao Y, Chow LH, Pickering JG. Evidence from a novel human cell clone that adult vascular smooth muscle cells can convert reversibly between noncontractile and contractile phenotypes. *Circ Res* 1999;85:338–48.
- [13] Sarkar S, Dadhania M, Rourke P, Desai TA, Wong JY. Vascular tissue engineering: microtextured scaffold templates to control organization of vascular smooth muscle cells and extracellular matrix. *Acta Biomater* 2005;1:93–100.
- [14] Shen JY, Chan-Park MB, He B, Zhu AP, Zhu X, Beuerman RW, et al. Three-dimensional microchannels in biodegradable polymeric films for control orientation and phenotype of vascular smooth muscle cells. *Tissue Eng* 2006;12(8):2229–40.
- [15] Shen JY, Chan-Park MBE, Feng ZQ, Chan V, Feng ZW. UV-embossed microchannel in biocompatible polymeric film: application to control of cell shape and orientation of muscle cells. *J Biomed Mater Res B Appl Biomater* 2006;77B(2):423–30.
- [16] Goessl A, Bowen-Pope DF, Hoffman AS. Control of shape and size of vascular smooth muscle cells in vitro by plasma lithography. *J Biomed Mater Res* 2001;57:15–24.
- [17] Glawe JD, Hill JB, Mills DK, McShane MJ. Influence of channel width on alignment of smooth muscle cells by high-aspect-ratio microfabricated elastomeric cell culture scaffolds. *J Biomed Mater Res* 2005;75:106–14.
- [18] Thakar RG, Cheng Q, Patel S, Chu J, Nasir M, Liepmann D, et al. Cell-shape regulation of smooth muscle cell proliferation. *Biophys J* 2009;96(8):3423–32.
- [19] Cao Y, Poon YF, Feng J, Rayatpisheh S, Chan V, Chan-Park MB. Regulating orientation and phenotype of primary vascular smooth muscle cells by biodegradable films patterned with arrays of microchannels and discontinuous microwalls. *Biomaterials* 2010;31:6228–38.
- [20] Chamley-Campbell JH, Campbell GR, Ross R. Phenotype-dependent response of cultured aortic smooth muscle to serum mitogens. *J Cell Biol* 1981;8:379–83.
- [21] Lagna G, Ku MM, Nguyen PH, Neuman NA, Davis BN, Hata A. Control of phenotypic plasticity of smooth muscle cells by bone morphogenetic protein signaling through the myocardin-related transcription factors. *J Biol Chem* 2007;282(51):37244–55.
- [22] Shioi A, Nishizawa Y, Jono S, Koyama H, Hosoi M, Morii H. Beta-glycerophosphate accelerates calcification in cultured bovine vascular smooth muscle cells. *Arterioscler Thromb Vasc Biol* 1995;15:2003–9.
- [23] Kennard S, Liu H, Lilly B. Transforming growth factor-beta (TGF-beta1) down-regulates notch3 in fibroblasts to promote smooth muscle gene expression. *J Biol Chem* 2008;283:1324–33.
- [24] Sinha S, Hoofnagle MH, Kingston PA, McCanna ME, Owens GK. Transforming growth factor-beta1 signaling contributes to development of smooth muscle cells from embryonic stem cells. *Am J Physiol Cell Physiol* 2004;287:1560–8.
- [25] Rama A, Matsushita T, Charolidi N, Rothery S, Dupont E, Severs NJ. Up-regulation of connexin43 correlates with increased synthetic activity and enhanced contractile differentiation in TGF-beta-treated human aortic smooth muscle cells. *Eur J Cell Biol* 2006;85:375–86.
- [26] Narita Y, Yamawaki A, Kagami H, Ueda M, Ueda Y. Effects of transforming growth factor-beta 1 and ascorbic acid on differentiation of human bone-marrow-derived mesenchymal stem cells into smooth muscle cell lineage. *Cell Tissue Res* 2008;333:449–59.
- [27] Deaton RA, Su C, Valencia TG, Grant SR. Transforming growth factor-beta1-induced expression of smooth muscle marker genes involves activation of PKN and p38 MAPK. *J Biol Chem* 2005;280(35):31172–81.
- [28] Sobue K, Hayashi K, Nishida W. Expressional regulation of smooth muscle cell-specific genes in association with phenotypic modulation. *Mol Cell Biochem* 1999;190:105–18.
- [29] Small JV, Gimona M. The cytoskeleton of the vertebrate smooth muscle cell. *Acta Physiol Scand* 1998;164:341–8.
- [30] DeFeo TT, Morgan KG. Responses of enzymatically isolated mammalian vascular smooth muscle cells to pharmacological and electrical stimuli. *Pfluegers Arch* 1985;404:100–2.
- [31] Ma H, Hyun J, Zhang Z, Beebe Jr TP, Chilkoti A. Fabrication of biofunctionalized quasi-three-dimensional microstructures of a nonfouling comb polymer by soft lithography. *Adv Funct Mater* 2005;15(4):529–40.
- [32] Zhao Y, Xiao H, Long W, Pearce WJ, Longo LD. Expression of several cytoskeletal proteins in ovine cerebral arteries: developmental and functional considerations. *J Physiol* 2004;558(2):623–32.
- [33] Chamley JH, Campbell GR, McConnell JD, Groschel-Stewart U. Comparison of vascular smooth muscle cells from adult human, monkey and rabbit in primary culture and in subculture. *Cell Tissue Res* 1977;177(4):503–22.
- [34] Hautmann MB, Madsen CS, Owens GK. A transforming growth factor beta (TGFbeta) control element drives TGF beta-induced stimulation of smooth muscle alpha-actin gene expression in concert with two CArG elements. *J Biol Chem* 1997;272(16):10948–56.
- [35] Finlay HM, Dixon JG, Canham PB. Fabric organization of the subendothelium of the human brain artery by polarized-light microscopy. *Arterioscler Thromb Vasc Biol* 1991;11:681–90.
- [36] Orlandi A, Bochaton-Piallat M-L, Gabbiani G, Spagnoli LG. Aging, smooth muscle cells and vascular pathobiology: implications for atherosclerosis. *Atherosclerosis* 2006;188:221–30.
- [37] Grainger DJ, Kemp PR, Metcalfe JC, Liu AC, Lawn RM, Williams NR, et al. The serum concentration of active transforming growth factor-beta is severely depressed in advanced atherosclerosis. *Nat Med* 1995;1:22–33.
- [38] Lutgens E, Gijbels M, Smook M, Heeringa P, Gotwals P, Koteliansky VE, et al. Transforming growth factor-beta mediates balance between inflammation and fibrosis during plaque progression. *Arterioscler Thromb Vasc Biol* 2002;22(6):975–82.
- [39] Majesky MW, Lindner Y, Twardzik DR, Schwartz SM, Reidy MA. Production of transforming growth factor beta 1 during repair of arterial injury. *J Clin Invest* 1991;88:904–10.
- [40] Stegemann JP, Nerem RM. Phenotypic modulation in vascular tissue engineering using biochemical and mechanical stimulation. *Ann Biomed Eng* 2003;31:391–402.
- [41] Neidert MR, Lee ES, Oegema TR, Tranquillo RT. Enhanced fibrin remodeling in vitro with TGF-beta1, insulin and plasmin for improved tissue equivalents. *Biomaterials* 2002;23(17):3717–31.
- [42] Wrana JL, Attisano L, Wieser R, Ventura F, Massague J. Mechanism of activation of the TGF-beta receptor. *Nature* 1994;370:341–7.
- [43] Nakao A, Imamura T, Souchelnytskyi S, Kawabata M, Ishisaki A, Oeda E, et al. TGF-beta receptor-mediated signaling through smad2, smad3, and smad4. *EMBO J* 1997;16(17):5353–62.
- [44] Holycross BJ, Blank RS, Thompson MM, Peach MJ, Owens GK. Platelet-derived growth factor-BB-induced suppression of smooth muscle cell differentiation. *Circ Res* 1992;71:1525–32.